

Research Article

Thermodynamic Analysis of the Hydrogen Production from Ethanol: First and Second Laws Approaches

Yannay Casas-Ledón,^{1,2} Luis E. Arteaga-Perez,¹
Mayra C. Morales-Perez,¹ and Luis M. Peralta-Suárez¹

¹Chemical Engineering Department, Central University of Las Villas, Carretera a Camajuani Km 5 y 1/2, Santa Clara, 54830 Villa Clara, Cuba

²Research Group ENVOG, Ghent University, Coupure Links 653, 9000 Ghent, Belgium

Correspondence should be addressed to Luis E. Arteaga-Perez, luiseap@uclv.edu.cu

Received 6 December 2011; Accepted 7 January 2012

Academic Editors: A. Ghoufi and P. Li

Copyright © 2012 Yannay Casas-Ledón et al. This is an open access article distributed under the Creative Commons Attribution License, which permits unrestricted use, distribution, and reproduction in any medium, provided the original work is properly cited.

A thermodynamic analysis of hydrogen production from ethanol steam reforming (ESR) is carried out in the present paper. The influence of reactants molar ratio feed into the reforming stage ($2.5 < \text{mol}_{\text{Water}}/\text{mol}_{\text{EtOH}} < 8$), temperature (573 to 1173 K) and pressure ($1 < P < 10$ atm) over equilibrium compositions is studied. The direct method employed to analyze the system is the minimization of Gibbs free energy (MGFE) in conjunction with Lee-Kesler state equation, using the Kay mixing rules. The temperature and reactants molar ratio showed a positive influence on the hydrogen yield; ethanol conversion is 100% for the whole interval analyzed while the pressure affected greatly the hydrogen production. The carbon deposition exhibits a maximum value at temperatures around 773 K, and three reactions are proposed to describe the solid carbon formation in a wide temperature range based on thermodynamics and experimental predictions. The conditioning stages (mixing, vaporization, and heating) are studied in addition to the reaction to analyze the system quality by means of an exergetic method applying the 2nd law of thermodynamic.

1. Introduction

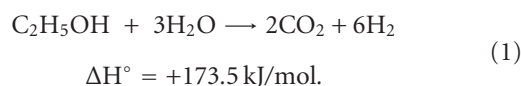
Steam reforming has been known since more than 100 years. For the past 50 years, its end product, syngas, has been used in the commercial production of fuels and chemicals mainly in the NH_3 industry. An attractive part of this technology is that it can accommodate a wide variety of gaseous, liquid, and solid feedstocks. When syngas production is coupled to an energy generation system, a high efficiency levels could be obtained; in this sense, the ethanol and biomass gasification to produce H_2 for fuel cells appears as a prominent alternative [1]. The main advantages in the use of Ethanol and biomass to produce hydrogen are supported on their renewable characteristics (it is part of a natural cycle), high yield in the production of hydrogen, easy handling, transportation, biodegradability, and null CO_2 emissions [2].

Nowadays there are several ways to produce hydrogen using ethanol as carrier material; the well-known reforming technologies are the main alternatives used in this sense;

in specific the steam reforming is the process that exhibits higher perspectives due to its efficiency, productivity, and implementation facilities [3].

Previous thermodynamics studies [4, 5] have shown that the ethanol steam reforming (e-s-r) is feasible to high temperatures ($T > 500$ K), being obtained as main products the CH_4 , H_2O , CO , CO_2 , and H_2 . Other H-C compounds as the acetaldehyde and the ethylene are considered intermediate products [6], which are quickly converted to more simple molecules at high contact times and temperatures; the production of these compounds over Ni^{2+} and Cu^{2+} sites was reported by Mariño et al. [7, 8].

According to the e-s-r stoichiometric, 6 mol of hydrogen would be produced for each ethanol molecule under conditions of 100% of conversion:



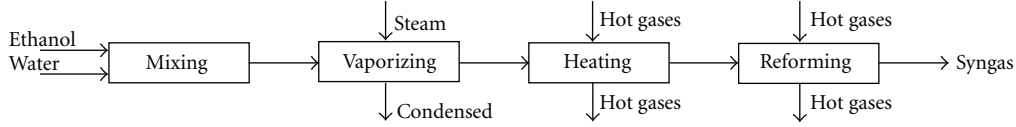
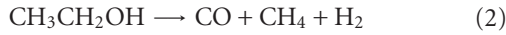


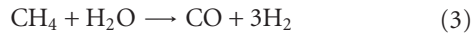
FIGURE 1: Simplified flow diagram of ethanol steam reforming.

In spite of the apparent simplicity of this reaction, under real conditions the process is more complex. There are several side-reaction pathways; some of which are favored by the catalysts bearing to the decrease of the productive efficiency. According to Comas et al. [9], when a Ni/Al₂O₃ catalyst is used, the main reaction stages are the following ones:

ethanol decomposition:



methane steam reforming:



ethanol steam reforming:



Although the catalytic formulation and the operational conditions affect strongly the reaction mechanism, when it's sought to approach the problem from the thermodynamic point of view the election of the equilibrium compounds is the decisive step to obtain a more realistic picture of the phenomenon. In this sense an independent system of reactions could be used to represent the e-s-r; the proposed scheme in this paper conceives the existence of (*i*) species at the equilibrium conditions [CO, (*i* = 1)-CO₂, (*i* = 2)-H₂, (*i* = 3)-CH₄, (*i* = 4)-H₂O, (*i* = 5)], considering that the process takes place to high temperatures (573 K < *T* < 1173 K).

In the present paper the thermodynamic analysis of the system is developed using the Gibbs free energy minimization method, which has been applied to similar systems by several authors [4, 10, 11]; as a novel concept this method is used together with the exergy analysis of the whole system represented in Figure 1 to evaluate the efficiency and the irreversibilities losses, giving a measure of the process quality relative to the use of the useful energy.

This procedure allows obtaining a real characterization of what happens in the process, and it's an important tool to evaluate the efficiency and irreversibility losses in all stages. Note that all the calculations are approximated to equilibrium and no kinetic assumptions are taken into consideration.

The H₂ production process from e-s-r is represented by 4 fundamental stages (Figure 1): blending, vaporization, heating, and reaction. The system is analyzed assuming an ethanol molar flow of 1 mol·s⁻¹.

2. Thermodynamic Analysis and Chemical Equilibrium Calculations

To determine the compositions of the chemical species at the equilibrium in the reaction stage (e-s-r), the minimization of the Gibbs free energy (ΔG_f°) method (MGFE) was used. Complex numerical solutions became within the method mentioned previously and the use of highly fast computing techniques is required for its solution.

The general MGFE method, as Arteaga et al. [12] outline, is based on minimizing the expression of the total Gibbs free energy of the reacting system, this consists on finding the values of the each equilibrium mols for all chemical species, when the total free energy of the system reaches its minimum value at a given temperature and pressure, keeping in mind the species mass balance constraints. The mathematical solution of this problem is based on Lagrange's multipliers method.

The Kotas [13] state equation was used to calculate the fugacity coefficients for each component in the gaseous mixture as a modification to the method described above:

$$\ln \varphi_i = Z - 1 - \ln(Z) + \frac{B}{V_r} + \frac{C}{2V_r^2} + \frac{D}{5V_r^5} + E, \quad (5)$$

where V_r is the reduced volume, Z , the compressibility factor and (B , C , D and E) are the virial coefficients, which can be calculated according to the following equations:

$$\begin{aligned} B &= b_1 - \frac{b_2}{T_r} - \frac{b_3}{T_r^2} - \frac{b_4}{T_r^3}, \\ C &= c_1 - \frac{c_2}{T_r} + \frac{c_3}{T_r^3}, \\ D &= d_1 + \frac{d_2}{T_r}, \\ E &= \frac{c_4}{2T_r^3 \gamma} \left\{ \beta + 1 - \left(\beta + 1 + \frac{\gamma}{V_r^2} \right) \exp\left(-\frac{\gamma}{V_r^2}\right) \right\}, \end{aligned} \quad (6)$$

where $b_1, b_2, b_3, b_4, c_1, c_2, c_3, d_1, d_2, \beta$, and γ are constants corresponding to the simple and reference fluids (Table 1).

The compressibility factor is calculated as a function of the reduced temperature, pressure, and the acentric factor (w).

TABLE 1: Values of the constants in (6).

Constants	Simple fluid	Reference fluid
b_1	0.1181193	0.2026579
b_2	0.265728	0.331511
b_3	0.154790	0.027655
b_4	0.030323	0.203488
c_1	0.0236744	0.0313385
c_2	0.0186984	0.0503618
c_3	0.0	0.016901
c_4	0.042724	0.041577
$d_1 \times 10^4$	0.155488	0.48736
$d_2 \times 10^4$	0.623689	0.0740336
β	0.65392	1.226
γ	0.060167	0.03754

For mixtures of gasses, this factor is calculated using the mixing rules of Lee and Kesler [14] represented by the following equations:

$$Z = Z^{(O)}(T_r, P_r) + \frac{\omega}{\omega^{(r)}} \left[Z^{(r)}(T_r, P_r) - Z^{(O)}(T_r, P_r) \right],$$

$$Z_{ci} = 0.02905 - 0.085\omega_i,$$

$$\omega = \sum_j x_j \omega_j,$$

$$V_{ci} = \frac{Z_{ci} R T_{ci}}{P_{ci}}, \quad (7)$$

$$T_c = \frac{1}{8V_c} \sum_j \sum_k x_j x_k \left(V_{cj}^{1/3} + V_{ck}^{1/3} \right)^3 \sqrt{T_{cj} T_{ck}},$$

$$P_c = \frac{Z_c R T_c}{V_c} = (0.2905 - 0.085\omega) \frac{R T_c}{V_c},$$

where V_c , T_c and P_c , are the critic values of volume, temperature and pressure.

2.1. Application of the MGFE to Ethanol Steam Reforming. The influence of the temperature, the reactants feed molar ratio H_2O /ethanol, and the pressure over products yields for the e-s-r was studied using the MGFE. The yield of each specie ($i = 1$ to 5) was determined following the definition (8) proposed by smith et al. [15].

$$Y_i = \frac{F_i^{\text{out}}}{F_{\text{Etanol}}^{\text{in}}}, \quad (8)$$

$$C_2H_6O : \frac{\Delta G_f^o}{R * T} + \text{Ln} \left(\frac{n_{C_2H_6O}}{\sum ni} \right) + \text{Ln}(P) + \text{Ln}(\varphi_i) + \frac{2\lambda_C}{R * T}$$

$$+ \frac{6\lambda_H}{R * T} + \frac{\lambda_O}{R * T} = 0, \quad (9)$$

$$H_2O : \frac{\Delta G_f^o}{R * T} + \text{Ln} \left(\frac{n_{H_2O}}{\sum ni} \right) + \text{Ln}(P) + \text{Ln}(\varphi_i) + \frac{2\lambda_H}{R * T}$$

$$+ \frac{\lambda_O}{R * T} = 0, \quad (10)$$

$$CH_4 : \frac{\Delta G_f^o}{R * T} + \text{Ln} \left(\frac{n_{CH_4}}{\sum ni} \right) + \text{Ln}(P) + \text{Ln}(\varphi_i) + \frac{\lambda_C}{R * T}$$

$$+ \frac{4\lambda_H}{R * T} = 0, \quad (11)$$

$$CO_2 : \frac{\Delta G_f^o}{R * T} + \text{Ln} \left(\frac{n_{CO_2}}{\sum ni} \right) + \text{Ln}(P) + \text{Ln}(\varphi_i) + \frac{\lambda_C}{R * T}$$

$$+ \frac{2\lambda_O}{R * T} = 0, \quad (12)$$

$$CO : \frac{\Delta G_f^o}{R * T} + \text{Ln} \left(\frac{n_{CO}}{\sum ni} \right) + \text{Ln}(P) + \text{Ln}(\varphi_i) + \frac{\lambda_C}{R * T}$$

$$+ \frac{\lambda_O}{R * T} = 0, \quad (13)$$

$$H_2 : \text{Ln} \left(\frac{n_{H_2}}{\sum ni} \right) + \text{Ln}(P) + \text{Ln}(\varphi_i) + \frac{2\lambda_H}{R * T} = 0, \quad (14)$$

$$C : 2n_{C_2H_6O} + n_{CH_4} + n_{CO_2} + n_{CO} = n_o C, \quad (15)$$

$$H : 6n_{C_2H_6O} + 4n_{CH_4} + 2n_{H_2O} + n_{H_2} = n_o H, \quad (16)$$

$$O : n_{C_2H_6O} + n_{H_2O} + 2n_{CO_2} + n_{CO} + 2n_{O_2} = n_o O, \quad (17)$$

$$\sum ni = n_{C_2H_6O} + n_{CH_4} + n_{CO_2} + n_{CO} + n_{H_2O} + n_{H_2} + n_{O_2}, \quad (18)$$

$n_o C$, is carbon, hydrogen, and oxygen feed.

ΔG_f^o and φ_i are the formation free energies and fugacity coefficients of each compound.

The carbon formation within catalysts pellets is one of the main problems in the steam reforming technology, because of this, the solid carbon formation gas phase reactions are taken into consideration in the present paper using a procedure similar to that reported by Lwin et al., (2000) [16], which considers the use of the phase equilibrium established between solid and vapor carbon in the gas phase [15]:

$$\overline{G}C_{(g)} = \overline{G}C_{(s)} \quad (19)$$

Being the Gibbs free energy function of the equilibrium condition for solid carbon,

$$\min(nG) = \sum_{i=1}^{NG} n_i \overline{G}_i + (n\overline{G})C_{(s)} \quad (20)$$

NG is the number of substances present in the gas phase while carbon is present in the solid phase, this equation is included in the total Gibbs function.

Finally a comparison of the thermodynamic predictions for carbon formation with an experimental data obtained

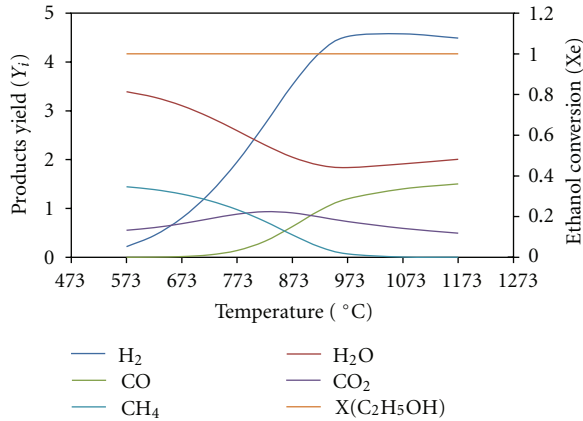


FIGURE 2: Temperature influence on products yield, pressure 1 atm, $H_2O/EtOH = 3.5 : 1$, ethanol flow = $1 \text{ mol} \cdot \text{s}^{-1}$.

in a pilot scale reactor is established, being demonstrated that the solid carbon deposition can be explained by three equilibrium reactions.

2.2. Results and Discussion of MGFE. The influence of the temperature (573 K to 1173 K) on the product yields considering a feed molar flow of ethanol of $1 \text{ mol} \cdot \text{s}^{-1}$, atmospheric pressure, and water-to-ethanol molar ratio of 3.5:1 is determined, being demonstrated that the products concentrations at equilibrium conditions are strongly affected by reaction temperature (Figure 2). In the whole interval it is observed that the ethanol reacts completely ($X_e = 100\%$); these results are in agreement with the experimental reports published elsewhere [3, 5, 15].

The hydrogen yield is increased approximately until a maximum value to 973 K due to the thermodynamics limitations of this system, which coincides with the total conversion of methane. The yields of H_2O , CO_2 , and CH_4 fall with the temperature, while those of CO are increased being proportional to the growth of hydrogen. This picture allows assuming that at higher temperatures the e-s-r is more feasible and the WGSR is a very probable reaction ($K_{eq} = 1.45$), also in a recent paper Arteaga et al. [12] shows a similar behavior of the hydrogen yield for temperatures above 973 K. The temperature seems to be always favorable for the process productivity, however in real processes this variable needs to be controlled in order to achieve catalyst specifications and avoid activity losses by means of catalyst sintering.

Figure 3 shows the effect of water-to-ethanol molar ratios (2.5:1 to 8:1) on products yield at 773 K and atmospheric pressure. In the whole studied range, ethanol reacts totally ($X_e = 100\%$), similar to the temperature behavior.

An increase in the water concentration fed into the reactor favors clearly the hydrogen production; this is related with H atoms included within water molecule that is to say the mass effect. On the other hand drastic decrease of the CH_4 yield is observed, mainly related with Le Chatelier's principle applied to the reforming CH_4 reaction which is highly favored by the water content in the reacting mixture. It could be inferred that the use of high concentrations of

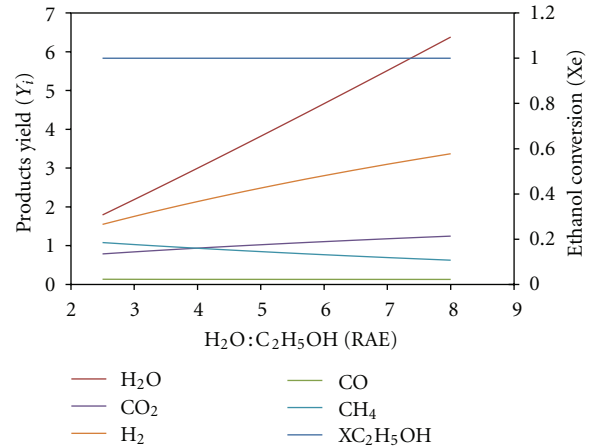


FIGURE 3: Effect of water/ethanol molar ratio on ethanol conversion and products yield, $P = 1 \text{ atm}$, $T = 773 \text{ K}$, and ethanol molar flow $1 \text{ mol} \cdot \text{s}^{-1}$.

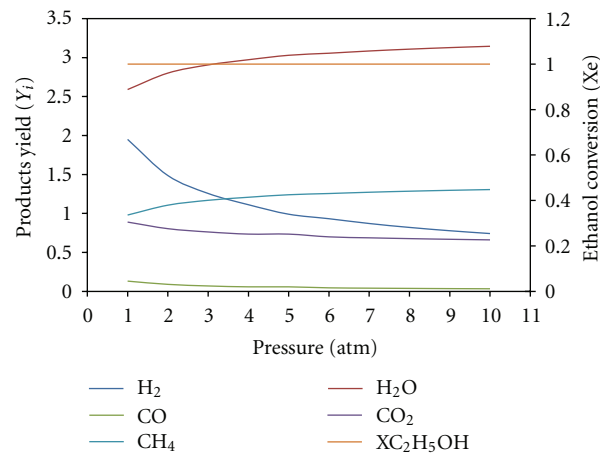


FIGURE 4: Pressure effects on Ethanol conversion and products yield, $H_2O/Ethanol = 3.5$, $T = 773 \text{ K}$ and ethanol flow $1 \text{ mol} \cdot \text{s}^{-1}$.

water is a decisive and positive factor to obtain high-quality performances, however this benefit could cause an increment of the energy costs in the previous vaporization and heating stages respectively, because of that in real system the efficient use of the energy needs to be controlled.

The simulation results in terms of the reaction pressure are represented in Figure 4. It is observed that an increment in the pressure reduces notably the hydrogen yield due to the expansion reactions involved in the steam reforming stage. This means that operation at high pressures affects severely the production process and due to this the exergetic analysis developed below is based on low pressures indexes.

Figure 5 shows the carbon deposition as a function of temperature. The dashed lines represent the theoretical predictions of solid carbon while the solid line represents experimental data measured in a pilot reactor of 1·10 m of length heated with three electric ovens equipped with several chromel-alumel slide thermocouples to control the temperature profiles along the bed. The gase compositions

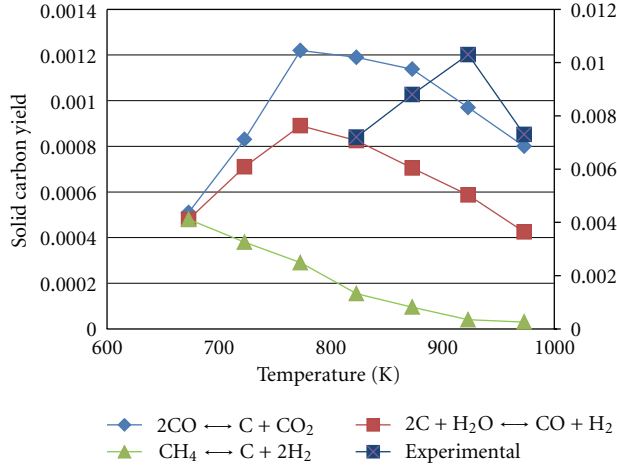
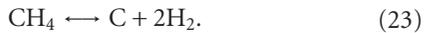
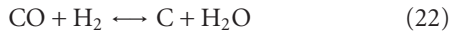


FIGURE 5: Effect of temperature on carbon deposition. Equilibrium and experimental data.

were measured with an Agilent 6820 gas chromatograph using FID and TCD detectors and the carbon deposition calculated with a mass balance restriction.

Both the theoretical and the experimental curves present a maximum at some temperature value between 773 K and 873 K. This fact may be related with the exothermic Boudouard reaction (21) and the reversible gasification of carbon (22), which are thermodynamically favorable at low temperatures, due to the high values of the equilibrium constant at those conditions while the reduction of the coke formation at temperatures above 873 K can be explained by the reverse gasification of carbon and the methane decomposition reaction (23) which competes with the methane steam reforming at these conditions (more feasible at high water to ethanol ratios):



Those results are coherent also with other experimental reports published elsewhere [17–19] and allow the reader to design experiments to establish the secure noncarbon deposition conditions.

3. Exergy Analysis

The exergy is defined as the maximum work that can be made by the components of a system regarding a reference system (usually the atmosphere), which is assumed to be infinite and in balance to a pressure, temperature, and defined chemical composition [13]. The exergy is a thermodynamic property that is determined by the system at atmosphere conditions; it is conserved just when the processes between the system and the atmosphere are reversible, and as well is destroyed when the processes are irreversible [11]. Because of the mentioned above the exergy analysis is very useful when the perfection

TABLE 2: Reference state compositions and species standard exergy.

Chemical species	Composition of the reference state (vol%)	Standard chemical exergy (J mol ⁻¹)
H ₂ O (g)	6.00	11710
H ₂ O (l)	—	3120
CO ₂	0.0329	20140
N ₂	73.40	720.0
O ₂	19.70	3970
CH ₄	—	836510
CO	—	275430
H ₂	—	238490
C ₂ H ₆ O (g)	—	1370800
C ₂ H ₆ O (l)	—	1364560
Total	100%	

of a real process needs to be studied, that is, to say that the exergy efficiency is more accurate and gives a better idea of the system than the simple energy efficiency.

The exergy could be considered as the sum of two components: physical exergy and chemical exergy. The work produced by a reversible process from its initial state (T, P) until the reference state (T_o, P_o) is known as physical exergy and can be calculated by means of 32:

$$E_{\text{ph}} = H - H_o - T_o(S - S_o), \quad (24)$$

where H, H_o and S, S_o are the enthalpy and entropy of each component at system conditions and to the reference state respectively.

This postulate shows clearly that the exergy is a property which is a function of the substance and the reference states. The temperature and pressure at the reference state in the present paper are set equal to $T_o = 298$ K and $P_o = 1.013$ atm respectively.

The work produced when a substance is changed from pressure and temperature conditions of the reference state until the chemical equilibrium state with the concentrations of the components at the reference, is known as chemical exergy. Due to this and considering that in the analyzed system the flows are mixtures in liquid (mixing stage) and gaseous states, the mathematical expression used to obtain the liquid mixture exergy is as follows:

$$E_{\text{ch}} = \sum_i x_i \cdot E_{\text{ch}_i}^o + R \cdot T_o \sum_i x_i \cdot \ln(\gamma_i \cdot x_i). \quad (25)$$

Equation (25) could be generalized for mixtures of gasses switching the activity to the volatility coefficient. When gaseous mixtures are studied under low pressures levels and the fugacity coefficients are very close to the unity (between 0.99 and 1.006 approximately) as in the present work, ideal behavior could be considered. In the present paper UNIQUAC method is used to obtain the activity coefficients according to the methodology proposed by Smith et al. [15]. The assumed reference state compositions and standard exergy of all species are showed in the Table 2.

The perfection degree of the process is determined using the exergy efficiency and losses criterions.

Exergy Efficiency (η_{Ex}). Exergy efficiency is an alternating way of measuring the appropriate use of the exergetic resources, to use this criterion adequately, it is necessary to identify the flows that are in interaction with the system. These interacting flows are known as “product” and “fuel” respectively, that is to say, the total exergy of entrance and the total exergy of the exit. Under these definitions, the exergy efficiency is the ratio between the exit and the entrance flows:

$$\eta_{\text{ex}} = \frac{E_p}{E_f} = 1 - \frac{E_d + E_l}{E_f}, \quad (26)$$

where E_D is the exergy destruction rate and E_L the exergy losses rate. E_P and E_F are exergy entrance and exit, respectively.

The exergy efficiency indicates what part of exergy that is fed into the system remains at the end of the process.

Exergy Losses (I). Exergy losses provide the thermodynamic measure of the system inefficiency and could be determined by the following expression:

$$I = E_{x_e} - E_{x_s}, \quad (27)$$

where subscripts (e) and (s) are referred to the inlet and outlet of the system respectively.

Another method that can also be used to study the exergy losses is the well known Guye and Stodola’s equation [13].

$$I = T_o \cdot \Delta S. \quad (28)$$

3.1. Results and Discussion of Exergy Analysis. In the present section, an exergetic analysis of the ethanol steam reforming is performed including the calculation of the physical and chemical exergies of all streams, the efficiencies, and the irreversibility losses of the whole process. The study is developed following a step-by-step methodology making a particular emphasis on reaction conditions (temperatures between 573 K and 1173 K, reactants feed ratio from 2.5 : 1 up to 8 : 1, and a pressure of 1 atm).

3.1.1. Effect of the Reaction Temperature. The exergy efficiency and losses are represented in Figure 6 as a function of the reaction temperature from 573 to 1173 K and maintaining the pressure at 1 atm and the feed molar ratio ($\text{H}_2\text{O}/\text{EtOH}$) of 3.5 : 1.

The efficiency of the process is higher than 60% for the whole interval of temperatures. A minimum region can be observed near to the 773 K (65%), which is produced by a dual function related with the temperature gradient between the reference state and the heating conditions and between the reactant mixture and the heating medium (assumed hot gasses). At temperatures below 773 K, the irreversibilities on reforming unit also showed significant values, which are attributed to the gradient of temperature between fuel and hot gasses needed to achieve a constant profile in the reactor.

On the other hand, when temperature is increased a proportional effect is observed for irreversibility losses, reaching a maximum at 1173 K equivalent to 1200 kW; as

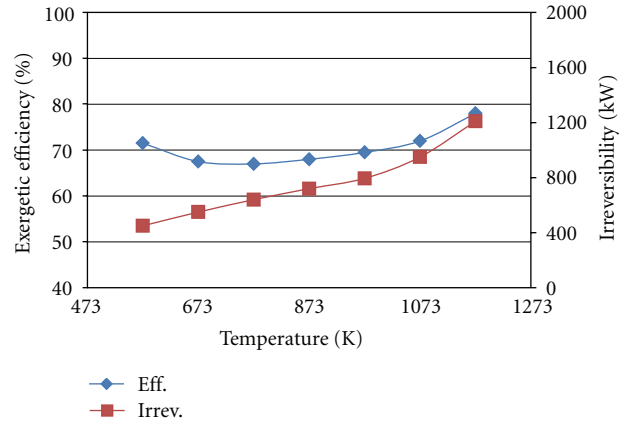


FIGURE 6: Influence of reaction temperature on exergy efficiency and losses, pressure 1 atm, $\text{H}_2\text{O}/\text{EtOH} = 3.5$.

TABLE 3: Exergy destruction in all process stages.

Temperature	Irreversibility, kW		
	573 K	773 K	1173 K
Mixing	2.98	2.98	2.98
Vaporization	206.23	206.23	206.23
Heating	113.67	298.45	1040.99
Reforming	201.72	158.10	12.04

can be corroborated (Table 3), the heating stage is the critical point of the system at high temperatures.

Taking into consideration that the studied process involves various highly energetic stages, a more detailed analysis is needed to determine which of these stages have bigger influence on the exergy destruction by irreversibility concept. The results obtained for 573 K, 773 K, and 1173 K are shown in Table 3.

The vaporization, heating, and reforming stages are the stages that higher irreversibility losses exhibited for the whole interval of temperatures. At 573 K the main losses are attributed to the vaporization and the reforming stages representing the 39.31 and 38.45%, respectively, followed by the heating unit where 21.66% of losses are expended.

At higher temperatures ($T > 773$ K), the main losses are observed in the heating stage increasing from 44.82% until 82.43%; on the other hand, the losses in the reformer diminished from 201.72 kW up to 12.04 kW at 1173 K. This decrease in the losses in the reaction stage is close related with the reaction efficiency which is a highly endothermic system and with the reduction of the temperature gradient between the fuel (reaction mixture) and the hot gasses used as heating medium.

The losses in the vaporization unit are associated to the phase change of the mixture water/ethanol from 298 K up to 367 K; as the composition of the mixture is not changed, the released exergy at this stage remains constant. It is worth to say that all the discussed above is referred to equilibrium calculations in all process stages so those are the maximum values to obtain in the process. A better picture of the process

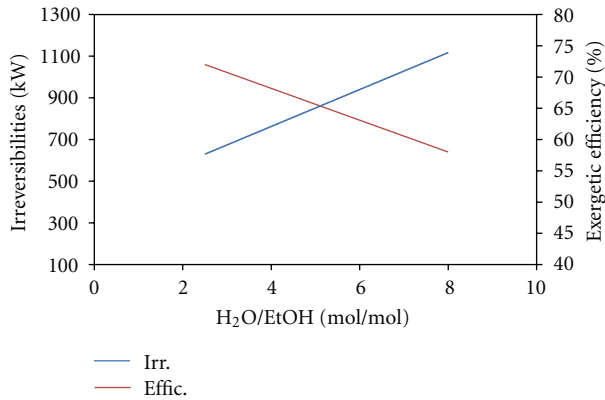


FIGURE 7: Effect of $H_2O/EtOH$ molar ratio on exergy efficiency and losses, $P = 1$ atm, and $T = 773$ K.

TABLE 4: Irreversibilities in all process stages. Reactants molar ratio effect.

Water/ethanol	Irreversibility, kW		
	2.5	4	8
Mixing	2.67	3.12	3.96
Vaporization	163.96	225.65	388.02
Heating	229.34	333.03	609.34
Reforming	168.05	154.21	125.16

could be obtained by using kinetic models in the ethanol steam reforming reactor and including the heat losses by heat transfer phenomena in all the heating units.

3.1.2. Effect of the Reactants Molar Ratio $H_2O/Ethanol$. The analysis of the second law applied to the e-s-r system is also carried out for different feeding reactants molar ratios $H_2O/ethanol = 3:1$ to $8:1$ at 773 K and constant pressure (1 atm). As it is illustrated in Figure 7, the exergy efficiency falls slightly with $H_2O/Ethanol$ ratios. On the other hand, the irreversibility indexes grow notably from 500 kW up to 1200 kW for change in composition of the reacting mixture of 75 to 88.9% mol respectively.

The growing behavior of the losses with water/ethanol molar ratios is due to the change in water composition (from 71.4 to 88.9% mol), which affects strongly the boiling point of the reacting mixture; that is to say, as this ratio increases the energy consumption involved in the stage of vaporization and heating of the mixture water-ethanol will be high. The increment in the water content produces a direct effect in the total flow because the ethanol feeding flow is constant and equal to $1 \text{ mol} \cdot \text{s}^{-1}$ for the whole interval of water/ethanol ratio studied, and, because of this, the sensible heat consumed in all process stages is proportional to the molar ratio used.

The above mentioned can be corroborated; if Table 4 is analyzed it is observed evidently, that the stages of more losses in the process are the vaporizer and the heater, both affected by the change in composition and molar flow of feed reactants.

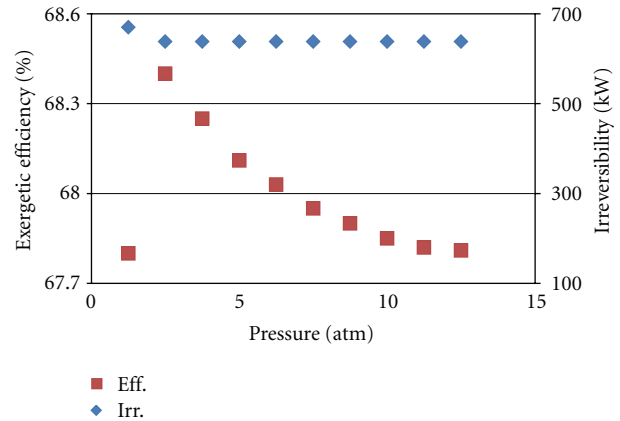


FIGURE 8: Pressure influence on efficiency and exergy losses. $H_2O/EtOH = 3.5$ and temperature 773 K.

TABLE 5: Irreversibilities in all process stages. Pressure effects.

Pressure	Irreversibility, kW		
	1 atm	5 atm	10 atm
Mixing	2.98	2.98	2.98
Vaporization	206.23	206.23	206.23
Heating	298.45	298.45	298.45
Reforming	158.1	153.88	157.99

3.1.3. Effect of the Reacting Pressure. The exergetic efficiency and exergy losses as a function of the reacting pressure when this is varied from 1 to 10 atm are represented in Figure 8, maintaining the reformer temperature and reactants molar ratio constants (773 K and $3.5:1$, resp.).

The operating pressure has not a marked influence on the exergy efficiency and losses because it is too close to the reference state. The difference of efficiency between the maximum point and minimum corresponding to 2 and 1 atm is about 1% , this can be corroborated by the results exposed in Figure 8, and the same behavior is showed by irreversibilities which present a plateau at 650 kW for all pressures. A clearer picture of irreversibilities in each stage of the process is depicted in Table 5 where it can be corroborated that this parameter is almost constant for all pressures studied; this behavior coincides directly in those reported in Figure 8 for reaction stage.

4. Conclusions

The thermodynamic analysis of the ethanol steam reforming process has shown the maximum yields of hydrogen that can be obtained for different operation conditions (temperature, pressure, and reactants molar ratios). The temperature and reactants molar ratios increment favors the levels of hydrogen yield being obtained a maximum at 973 K for a $H_2O/ethanol$ of $3.5:1$. On the other hand, the pressure is a variable that affects highly the process performance. There is a group of three reactions (21)–(23) which can be used to describe the solid carbon deposition and to establish

the secure operation region where coke is not deposited on catalyst surface; the latter was proved using theoretical and experimental results. The quality of the system was studied by means of the exergy analysis beside identifying the stages of more irreversible losses, the system boundaries and the reference state play an important role on exergy losses and the efficiency values. The process integration and the heat reuse between the process stages could lead to an increase of the system efficiency. The temperature and the water/ethanol ratio had showed a marked incidence on the exergy efficiency, not happening with the pressure, which had a negligible influence on efficiency and exergy losses, due to the littler difference between the reference state and real process evaluated.

Acknowledgments

The authors wish to acknowledge to the editor and unknown referees. This work has been financially supported by the VLIR Program, Project 7 (Environmental Education and Development of Clean Technologies), Ghent University, Faculty of Bioscience Engineering, and the Catalytic Productions Laboratory of Universidad de Buenos Aires.

References

- [1] H. Y. Kim, "A low cost production of hydrogen from carbonaceous wastes," *International Journal of Hydrogen Energy*, vol. 28, no. 11, pp. 1179–1186, 2003.
- [2] S. D. Minteer, *Alcoholic Fuels: An Overview*, Taylor and Francis Group, Boca Raton, Fla, USA, 2007.
- [3] F. Marino, M. Boveri, G. Baronetti, and M. Laborde, "Hydrogen production via catalytic gasification of ethanol. A mechanism proposal over copper-nickel catalysts," *International Journal of Hydrogen Energy*, vol. 29, no. 1, pp. 67–71, 2004.
- [4] K. Vasudeva, N. Mitra, P. Umasankar, and S. C. Dhingra, "Steam reforming of ethanol for hydrogen production: thermodynamic analysis," *International Journal of Hydrogen Energy*, vol. 21, no. 1, pp. 13–18, 1996.
- [5] M. A. Laborde and E. Y. Garcia, "Hydrogen production by the steam reforming of ethanol: thermodynamic analysis," *International Journal of Hydrogen Energy*, vol. 16, no. 5, pp. 307–312, 1991.
- [6] I. Fishtik, A. Alexander, R. Datta, and D. Geana, "A thermodynamic analysis of hydrogen production by steam reforming of ethanol via response reactions," *International Journal of Hydrogen Energy*, vol. 25, no. 1, pp. 31–45, 2000.
- [7] F. Marino, M. Boveri, G. Baronetti, and M. A. Laborde, "Hydrogen production from steam reforming of ethanol using Cu/Ni/K/g-Al₂O₃ catalysts. Effect of Ni," *International Journal of Hydrogen Energy*, vol. 26, no. 7, pp. 665–668, 2001.
- [8] F. Marino, M. Boveri, G. Baronetti, and M. Laborde, "Hydrogen production via catalytic gasification of ethanol. A mechanism proposal over copper-nickel catalysts," *International Journal of Hydrogen Energy*, vol. 29, no. 1, pp. 67–71, 2004.
- [9] J. Comas, F. Marino, M. Laborde, and N. Amadeo, "Bio-ethanol steam reforming on Ni/Al₂O₃ catalyst," *Chemical Engineering Journal*, vol. 98, no. 1-2, pp. 61–68, 2004.
- [10] S. H. Chan and H. M. Wang, "Thermodynamic analysis of natural-gas fuel processing for fuel cell applications," *International Journal of Hydrogen Energy*, vol. 25, no. 5, pp. 441–449, 2000.
- [11] M. Rosen, "Second-law analysis: approaches and implications," *International Journal of Energy Research*, vol. 23, no. 5, pp. 415–429, 1999.
- [12] L. E. Arteaga, L. M. Peralta, V. Kafarov, Y. Casas, and E. Gonzalez, "Ethanol steam reforming for ecological syngas and electricity production using a fuel cell SOFC system," *Chemical Engineering Journal*, vol. 136, no. 2–3, pp. 256–266, 2007.
- [13] T. J. Kotas, *The Exergy Method of Thermal Plant Analysis*, Krieger, Malaba, Kenya, 1995.
- [14] B. Lee and M. Kesler, "A generalized thermodynamic correlation based on three-parameter corresponding states," *AIChE Journal*, vol. 21, no. 3, pp. 510–526, 1975.
- [15] M. S. Smith, H. C. Van Ness, and M. M. Abbot, *Introduction to Chemical Engineers Thermodynamics*, Chemical Engineering Series, McGraw-Hill, 7th edition, 2005.
- [16] Y. Lwin, W. R. Wan, A. B. Mohamad, and Z. Yaakob, "Hydrogen production from steam±methanol reforming: thermodynamic analysis," *International Journal of Hydrogen Energy*, vol. 25, no. 1, pp. 47–53, 2000.
- [17] V. Fierro, V. Klouz, O. Akdim, and C. Mirodatos, "Oxidative reforming of biomass derived ethanol for hydrogen production in fuel cell applications," *Catalysis Today*, vol. 75, no. 1–4, pp. 141–144, 2002.
- [18] S. Cavallaro, V. Chiodo, A. Vita, and S. Freni, "Hydrogen production by auto-thermal reforming of ethanol on Rh/Al₂O₃ catalyst," *Journal of Power Sources*, vol. 123, no. 1, pp. 10–16, 2003.
- [19] M. Benito, J. L. Sanz, R. Isabel, R. Padilla, R. Arjona, and L. Daza, "Bio-ethanol steam reforming: insights on the mechanism for hydrogen production," *Journal of Power Sources*, vol. 151, no. 1-2, pp. 11–17, 2005.



Hindawi

Submit your manuscripts at
<http://www.hindawi.com>

